Real Time Movement Classification in Versatile CPG Control

Melanie Jouaiti   **Patrick Henaff**
Université de Lorraine, CNRS, Inria, LORIA, F-54000 Nancy, France

Abstract

Everyday human tasks are composed of a succession of discrete and rhythmic movements. If we want robots to be able to interact appropriately, it appears paramount for them to be able to perform both types of movements too. Though Central Pattern Generators (CPGs) are usually employed for rhythmic movement generation, they are also able of producing discrete movements. In this paper, we present a classification method to distinguish rhythmic and discrete movements so that the CPG can switch from one mode to the other. Moreover, we introduce several new plasticity rules more suitable for discrete movements.

1 Introduction

Discrete movements are defined as singularly occurring events preceded and followed by a period without motion; rhythmic movements are continuous and recurring periodically. It was proposed that rhythmic movements might be a concatenation of discrete movements [Baratto et al., 1986, Feldman, 1980] or on the contrary, discrete movements might be aborted rhythmic movements [Mottet and Bootsma, 1999, Guiard, 1993]. A fMRI study by [Schaal et al., 2004] revealed that rhythmic movements involve only a subset of the cortical activity observed in discrete movements, effectively demonstrating that the neural mechanisms differ for rhythmic and discrete movements.

The distinction between rhythmic and discrete movements is still an ongoing problematic in motor neuroscience. Complex tasks involve a closely intertwined association of both discrete and rhythmic movements

(cleaning, piano playing...). While humans are naturally able to seamlessly combine rhythmic and discrete movements, this is a bigger issue in robotics. Robot controllers need to be able to realize both types of movements and easily transition from one mode to the other. Several such structures have already been proposed, they are mainly a combination of rhythmic and discrete pattern generators. [Degallier et al., 2011] introduced a model associating the Hopf (rhythmic) and VITE (discrete) [Bullock and Grossberg, 1988] models. In [Sternad et al., 2000], the Matsuoka (rhythmic) [Matsuoka, 1985] and VITE (discrete) models were combined together. [de Rugy and Sternad, 2003, Sternad, 2008] proposed a model based solely on the Matsuoka oscillator but the discrete movement generated is merely the abortion of a rhythmic movement. As underlined by [Degallier and Ijspeert, 2010], the Matsuoka oscillator is indeed intrinsically rhythmic and can't generate real discrete movements.

In [Jouaiti and Henaff, 2018], we showed that the Rowat-Selverston oscillating neuron model [Rowat and Selverston, 1993] is able to generate both rhythmic and discrete movements and seamlessly switch from one mode to the other. A high-level rationale to switch from one mode to the other was however lacking. This paper is thus an attempt to answer that question.

A CPG is a biological structure found in the spinal cord of vetebrates. It is responsible for the generation of rhythmic patterns which can be modulated by sensory feedbacks. CPG models are based on a pair of mutually inhibitory oscillating neurons, called half-center [Grillner and Wallen, 1985, Rybak et al., 2006], controlling the extensor and flexor muscles. Non-linear models of CPG, also called relaxation oscillators, can synchronize with an external input or with a coupled CPG, thus ensuring coordination. The model of CPG used here has four layers: Rhythm Generator, Pattern Formation, Sensory Neurons and Motoneurons and incorporate hebbian plasticity rules allowing versatility and adaptation. CPGs provide an control which allows to imitate movements but not copy them, so that each system (human and robot in Human-Robot Interactions) can retain their own characteristics while

coordinating. We observe the same phenomenon with humans who can imitate each other without exactly copying (e.g. different amplitude, different kind of movement). Moreover, CPGs are quite robust to aberrant values (e.g. punctual error in the input signal).

In this work, we revise the plasticity rules introduced in [Jouaiti et al., 2018] to make them effective for discrete movements too. We also propose a classification algorithm for rhythmic and discrete movements which has been implemented into the CPG so that the CPG can automatically switch from one mode to the other. We will demonstrate the effectiveness of this system using human motion data. In the first section, we will recall the CPG architecture and introduce the new plasticity rules and the classification algorithm. Then, we will present results demonstrating the effectiveness of the new learning mechanisms and classification. Finally, we will discuss our results.

2 Material and Method

In this section, we will first recall the CPG architecture. Then, we will introduce the new plasticity rules for the discrete mode. Finally, we will present our classification rule for rhythmic and discrete movements.

2.1 CPG Architecture

The general architecture for the CPG is represented Fig. 3. See [Jouaiti et al., 2018] for extensive details.

For the rhythm generator neurons, Rowat-Selverston cells are used, the neuron model can be written as follows:
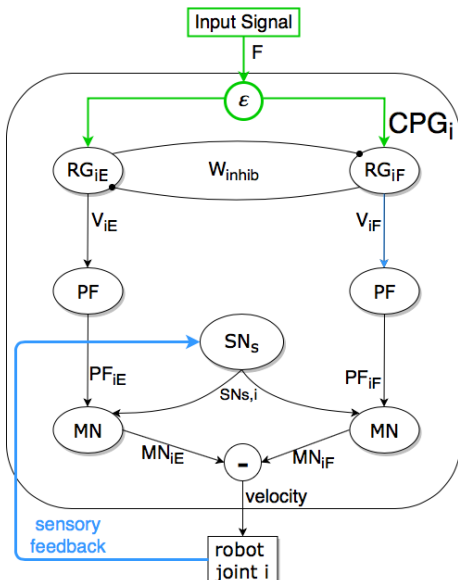

Figure 1: General CPG architecture. With $A(F)$ the amplitude of F

$$\dot{V}_{i_{\{E,F\}}} = y_{i_{\{E,F\}}} - W \frac{y_{i_{\{E,F\}}}}{1 + e^{-4y_{i_{\{F,E\}}}}} + \epsilon_{i_{\{E,F\}}} F_i \quad (1)$$

$$\dot{y}_{i_{\{E,F\}}} =$$

$$\left(\sigma_f - \frac{\tau_m}{\tau_s} - 1 - \sigma_f \tanh^2 \left(\frac{\sigma_f}{A_{f_{i_{\{E,F\}}}}} V_{i_{\{E,F\}}} \right) \right) \cdot$$

$$\frac{y_{i_{\{E,F\}}}}{\tau_m} - \frac{1 + \sigma_{s_{i_{\{E,F\}}}}}{\tau_s \tau_m} V_{i_{\{E,F\}}} +$$

$$\frac{A_{f_{i_{\{E,F\}}}}}{\tau_s \tau_m} \tanh \left(\frac{\sigma_f V_{i_{\{E,F\}}}}{A_{f_{i_{\{E,F\}}}}} \right) \quad (2)$$

with V the membrane potential and τ_m and τ_s time constants, A_f influences the output amplitude, while σ_f determines whether the neuron is able to oscillate or not. σ_s influences the intrinsic frequency, $i \in \mathbb{N}$, designating the joint id. F_i the CPG input, ϵ a synaptic weight designed to scale the input and the term in W models the mutual inhibition between the extensor and flexor rhythmic cells.

2.2 CPG Discrete Mode

The CPG can seamlessly switch from one mode to the other by modifying the values of σ_f and σ_s [Jouaiti and Henaff, 2018]. Setting $\sigma_f = 0.0$ and $\sigma_s \leq 1.0$ will yield a discrete mode and the CPG become equivalent to a PID controller. The rhythmic mode requires $\sigma_f \geq 1.0$ and $\sigma_s > 1$. However, the plasticity rules we introduced in [Jouaiti et al., 2018] were exclusively designed for the rhythmic mode and are not appropriate for discrete movements. Consequently, we modify the plasticity equations as follows:

The frequency learning rule which was previously defined follows:

$$\dot{\sigma}_{s_{i_{\{E,F\}}}} =$$

$$2\epsilon_{i_{\{E,F\}}} F_i \sqrt{\tau_m \tau_s (1 + \sigma_{s_{i_{\{E,F\}}}} - \sigma_f)} \cdot \frac{y_{i_{\{E,F\}}}}{\sqrt{V_{i_{\{E,F\}}}^2 + y_{i_{\{E,F\}}}^2}} \quad (3)$$

becomes:

$$\dot{\sigma}_{s_{i_{\{E,F\}}}} =$$

$$\sigma_F \cdot 2\epsilon_{i_{\{E,F\}}} F_i \sqrt{\tau_m \tau_s (1 + \sigma_{s_{i_{\{E,F\}}}} - \sigma_f)} \cdot \frac{y_{i_{\{E,F\}}}}{\sqrt{V_{i_{\{E,F\}}}^2 + y_{i_{\{E,F\}}}^2}} \quad (4)$$

This rule now ensures that frequency learning is disabled in discrete mode, i.e. when $\sigma_f = 0.0$.

The learning rule for A_F remains unchanged:

$$\dot{A}_{f_{i_{\{E,F\}}}} = -\mu \left(\left(\frac{\nu \sigma_f V_{i_{\{E,F\}}}}{A_{f_{i_{\{E,F\}}}}} \right)^2 - F_i^2 \right) \quad (5)$$

The equation for ϵ previously defined as:

$$\dot{\epsilon}_{i_{\{E,F\}}} = \lambda tanh^2(\xi F_i) \left(1 - (\epsilon_{i_{\{E,F\}}} F_i)^2 \right) \quad (6)$$

becomes:

$$\begin{aligned} \dot{\epsilon}_{i_{\{E,F\}}} = & \\ & tanh^2(\xi F_i) \cdot \\ & [(1 - \sigma_f) \cdot \lambda(F_i^2 - output_i^2) + \\ & \sigma_f \cdot \lambda(1.0 - (\epsilon \cdot F_i)^2)] \end{aligned} \quad (7)$$

This ensures that the amplitude of ϵF remains 1.0 (optimal functioning mode) in the rhythmic mode, while forcing the output amplitude to match the input amplitude in the discrete mode.

2.3 Rhythmic - Discrete Classification

To classify the signal as rhythmic or discrete, we use the Fast Fourier Transform (FFT) over n sliding windows of size $\{1, ..., n\}$ seconds. If the difference between the maximum of the FFT and the mean is large, then we assume that there is a frequency peak. We also consider the spread of the peak. Combining several window sizes also allows to take a wider range of frequency into account. This yields the following equation for $C(x,t)$ the classification result at time t with x the array of all input values:

$$C(x,t) = \sum_{N=1}^{n} P(\{x_{t-N}...x_t\}) + \alpha \cdot S(\{x_{t-N}...x_t\}) \quad (8)$$

$$P(x) = max(FFT(x)) - \overline{FFT(x)} - \\ stdDev(FFT(x)) \quad (9)$$

$$S(x) = len\left(FFT(x) > \overline{FFT(x)}\right) \quad (10)$$

with n the number of iterations, $FFT(x)$ the FFT of x, $stdDev(x)$ the standard deviation of x and

$len(FFT > \overline{FFT}$ the number of values greater than the average FFT.

This allows us to introduce a new synaptic rule for σ_f related to the rhythmic / discrete movement detection:

$$\dot{\sigma}_f = \gamma \cdot \left(\frac{\tanh(100.0 \cdot C(x,t)) + 1.0}{2.0} - \sigma_f \right) \quad (11)$$

with γ a learning step.

The classification results are positive for rhythmic movements and negative for discrete movements. The classification is amplified with a gain and smoothed and normalized using a sigmoid. According to this rule, σ_f converges towards 1 when the classification result is positive and towards 0 when it is negative.

3 Results

First, we will demonstrate the effectiveness of the new plasticity rule for ϵ. Then we will evaluate our classification algorithm. And finally, we will present results for σ_f learning mechanism.

3.1 Discrete Movements

To demonstrate the effectiveness of the new rule, we tested the model with systematic data: a step, a ramp and a sinusoid. We can observe on Figure 2 that although the CPG without learning effectively reproduces the signal, it doesn't match the amplitude of the signal. However, with the new learning rule for ϵ, the CPG also adapts to the input amplitude.
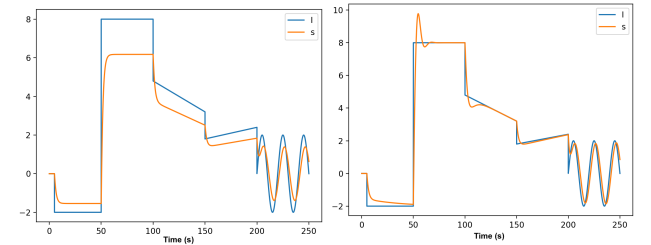

Figure 2: In blue: input signal of the CPG; in orange: CPG output. Left: CPG without any learning rule. Right: CPG with the new learning rule

3.2 Rhythmic - Discrete Movements Classification

The classification algorithm runs in average in 4 ms for each time step, allowing real time classification. The classification algorithm has been tested on human motion data acquired with the T-Sens Motion Sensors [tea,]. The participants were performing series of nine ten seconds waving followed each time by four to six seconds of rest. Sampling frequency was

$64Hz$. 4457.53 seconds of data were manually labelled as rhythmic or discrete and the classification was evaluated on this data.

Let us define precision, recall and F1-score as follows:

$$precision = \frac{TP}{TP + FP} \tag{12}$$

$$recall = \frac{TP}{TP + FN} \tag{13}$$

$$F = 2 \cdot \frac{precision \cdot recall}{precision + recall} \tag{14}$$

with TP the number of true positives, FP th enumber of false positives and FN the number of false negatives.

Overall, we obtained 65% ($\pm5\%$) of precision, 100% ($\pm6.2e^{-6}\%$) of recall and a F1 score of 0.79 (±0.04). Failures of classification mostly come from data which looks like noise and fails to be classified as rhythmic. Moreover, although the classification immediately detects a switch from discrete to rhythmic, there is a delay for the transition between rhythmic and discrete.
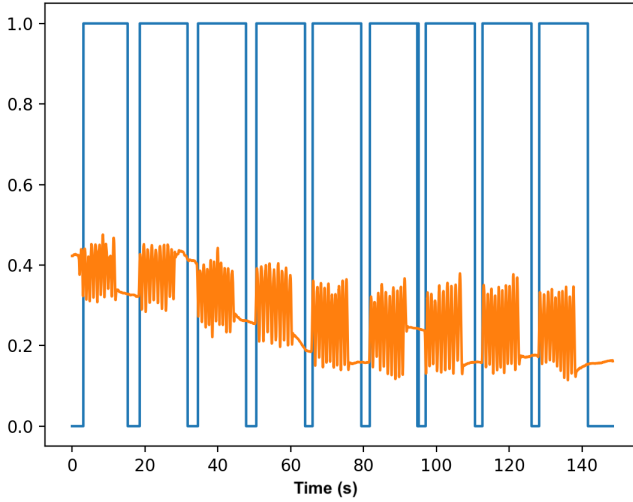

Figure 3: Example of classification result. In orange, the movement data, in blue, the classification result (1 for rhythmic and 0 for discrete)

3.3 CPG Adaptation

Combining the two previous parts, the CPG is now able to determine the type of input it is receiving and switch its parameters accordingly. We demonstrate this with the human motion previously classified in subsection 3.1. For this example, we achieve 64% precision, 100 % recall and a F1-score of 0.78.

We can see on Figure 4 that σ_f is able to adapt very quickly to changes between rhythmic and discrete

movements. We evaluate the CPG coordination ability using the Phase Locking Value (PLV). The PLV has been introduced by [Lachaux et al., 1999] to measure coordination in brain signals. It relies on the assumption that both signals are locked with a constant phase difference but the PLV allows for deviations and evaluates this spread. It ranges from 0 (no coordination) to 1 (perfect coordination):

$$PLV(t) = \frac{1}{N} \left| \sum_{i=0}^{N} e^{j(\phi_1(i) - \phi_2(i))} \right| \tag{15}$$

with N the sliding window size, $j = \sqrt{-1}$, ϕ_k the instantaneous phase of signal k.

It can be observed on Figure 5 that, while the PLV struggles at transitions, the signals are coordinated (high PLV score) most of the time.

Evaluating the performance on all the data yields an average PLV of 0.85 (±0.04), 62 % ($\pm3\%$) precision, 98% ($\pm7\%$) recall and a F1-score of 0.76 (±0.04).

4 Conclusion

In this work, we revised the plasticity rules introduced in [Jouaiti et al., 2018] to make them effective for discrete movements too. We also proposed a classification rule for rhythmic and rhythmic movements which has been implemented into the CPG so that the CPG can automatically switch from one mode with the other. We showed that the CPG is effectively able to adapt to both discrete and rhythmic movements using human motion data.

Though the results are not perfect, they are highly satisfactory, especially considering the variability in the input signals. In future work, we will validate this in real human-robot interactions where the robot will imitate the human movements.

This work also demonstrates the versatility of the Rowat-Selverston model which can incorporate a wide range of plasticity mechanisms. These mechanisms can be freely modified to take into account the constraints or goals of the interactions and expand the adaptive capabilities of the CPG.

References

[tea,] Captiv tea, france. http://teaergo.com/wp/.

[Baratto et al., 1986] Baratto, L., Morasso, P., and Zaccaria, R. (1986). Complex motor patterns: Walking. In *Advances in Psychology*, volume 33, pages 60–81. Elsevier.
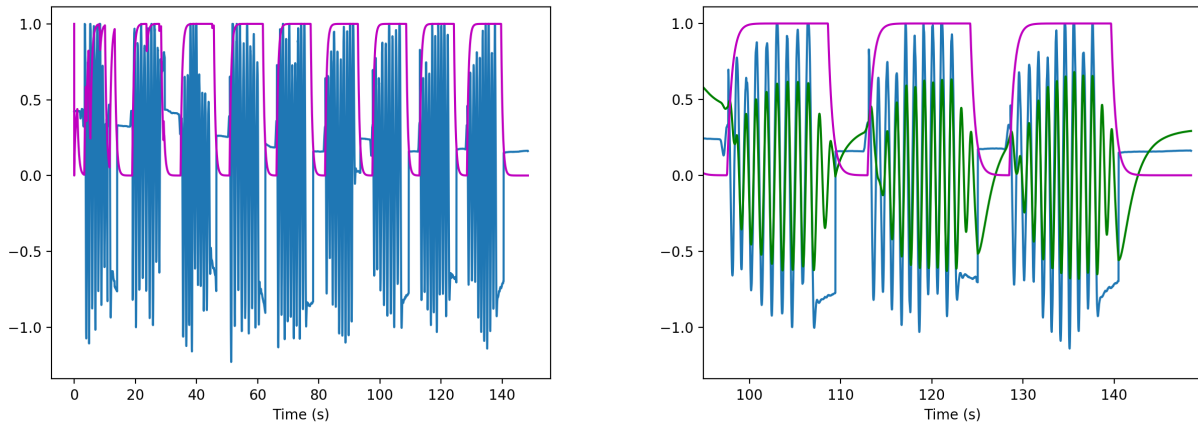
Figure 4: Left: Example of classification result. In blue, the CPG input, in magenta, the evolution of σ_f, i.e. classification result (1 for rhythmic and 0 for discrete). Right: Zoom over the results. In blue, the CPG input, in green the CPG output, in magenta, the evolution of σ_f
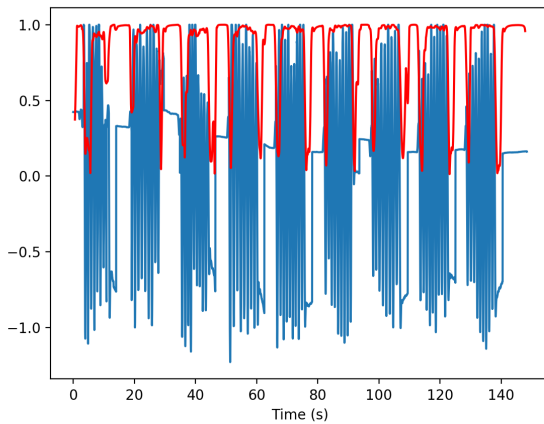

Figure 5: Coordination performance of the CPG (PLV between the CPG input and output). In blue, CPG input, in red, PLV score

[Bullock and Grossberg, 1988] Bullock, D. and Grossberg, S. (1988). The vite model: a neural command circuit for generating arm and articulator trajectories. *Dynamic patterns in complex systems*, pages 305–326.

[de Rugy and Sternad, 2003] de Rugy, A. and Sternad, D. (2003). Interaction between discrete and rhythmic movements: reaction time and phase of discrete movement initiation during oscillatory movements. *Brain Research*, 994(2):160–174.

[Degallier and Ijspeert, 2010] Degallier, S. and Ijspeert, A. (2010). Modeling discrete and rhythmic movements through motor primitives: a review. *Biological cybernetics*, 103(4):319–338.

[Degallier et al., 2011] Degallier, S., Righetti, L., Gay, S., and Ijspeert, A. (2011). Toward simple control for complex, autonomous robotic applications: combining discrete and rhythmic motor primitives. *Autonomous Robots*, 31(2-3):155–181.

[Feldman, 1980] Feldman, A. (1980). Superposition of motor programs—i. rhythmic forearm movements in man. *Neuroscience*, 5(1):81–90.

[Grillner and Wallen, 1985] Grillner, S. and Wallen, P. (1985). Central pattern generators for locomotion, with special reference to vertebrates. *Annual review of neuroscience*, 8(1):233–261.

[Guiard, 1993] Guiard, Y. (1993). On fitts's and hooke's laws: Simple harmonic movement in upper-limb cyclical aiming. *Acta psychologica*, 82(1-3):139–159.

[Jouaiti et al., 2018] Jouaiti, M., Caron, L., and Hénaff, P. (2018). Hebbian plasticity in cpg controllers facilitates self-synchronization for human-robot handshaking. *Frontiers in Neurorobotics*, 12:29.

[Jouaiti and Henaff, 2018] Jouaiti, M. and Henaff, P. (2018). Cpg-based controllers can generate both discrete and rhythmic movements. In *2018 IEEE/RSJ International Conference on Intelligent Robots and Systems (IROS)*.

[Lachaux et al., 1999] Lachaux, J.-P., Rodriguez, E., Martinerie, J., Varela, F. J., et al. (1999). Measuring phase synchrony in brain signals. *Human brain mapping*, 8(4):194–208.

[Matsuoka, 1985] Matsuoka, K. (1985). Sustained oscillations generated by mutually inhibiting neurons

with adaptation. *Biological cybernetics*, 52(6):367–376.

[Mottet and Bootsma, 1999] Mottet, D. and Bootsma, R. J. (1999). The dynamics of goal-directed rhythmical aiming. *Biological cybernetics*, 80(4):235–245.

[Rowat and Selverston, 1993] Rowat, P. F. and Selverston, A. I. (1993). Modeling the gastric mill central pattern generator of the lobster with a relaxation-oscillator network. *Journal of neurophysiology*, 70(3):1030–1053.

[Rybak et al., 2006] Rybak, I. A., Shevtsova, N. A., Lafreniere-Roula, M., and McCrea, D. A. (2006). Modelling spinal circuitry involved in locomotor pattern generation: insights from deletions during fictive locomotion. *The Journal of physiology*, 577(2):617–639.

[Schaal et al., 2004] Schaal, S., Sternad, D., Osu, R., and Kawato, M. (2004). Rhythmic arm movement is not discrete. *Nature neuroscience*, 7(10):1136.

[Sternad, 2008] Sternad, D. (2008). Towards a unified theory of rhythmic and discrete movements—behavioral, modeling and imaging results. In *Coordination: Neural, behavioral and social dynamics*, pages 105–133. Springer.

[Sternad et al., 2000] Sternad, D., Dean, W. J., and Schaal, S. (2000). Interaction of rhythmic and discrete pattern generators in single-joint movements. *Human Movement Science*, 19(4):627–664.